THE ENCYCLOPEDIA OF MATERIALS SCIENCE AND TECHNOLOGY

Editors-in-Chief

K.H. Jürgen Buschow Robert W. Cahn
Merton C. Flemings Bernhard Ilschner
Edward J. Kramer Subhash Mahajan

Subject editors

Continuous Parallel Fiber Composites: Fracture

The purpose of this article is to provide a brief overview of the micromechanics associated with fracture of unidirectional composites with particular emphasis on toughening mechanisms. Overload fracture is a common failure mode for high-strength, high-stiffness materials. Crack-like flaws are inevitably generated in a material either during fabrication or during service life. If the severity of the flaw is large or the load is high enough, then the flaw becomes the initiation site for catastrophic unstable fracture. A major advantage of composites, however, is that their microstructure promotes the accumulation of small flaws (damage), rather than the growth of a dominant crack. This mechanism of damage accumulation imparts significant energy dissipation capability or fracture toughness to the material, and is most exploited in brittle matrix composite systems.

Composites are most often classified in terms of their matrix, and are designated as polymer matrix composites (PMCs), metal matrix composites (MMCs), or ceramic matrix composites (CMCs). Although these systems possess widely different mechanical properties, they experience similar damage accumulation processes. More significantly, although damage introduces a high level of complexity in determining the stress field ahead of a crack tip or a notch, energy-based fracture mechanics concepts allow an elegant means of characterizing the condition for failure, which spans across all the three matrix systems. These issues on the mechanics and mechanisms of fracture of unidirectional composites are discussed in this article.

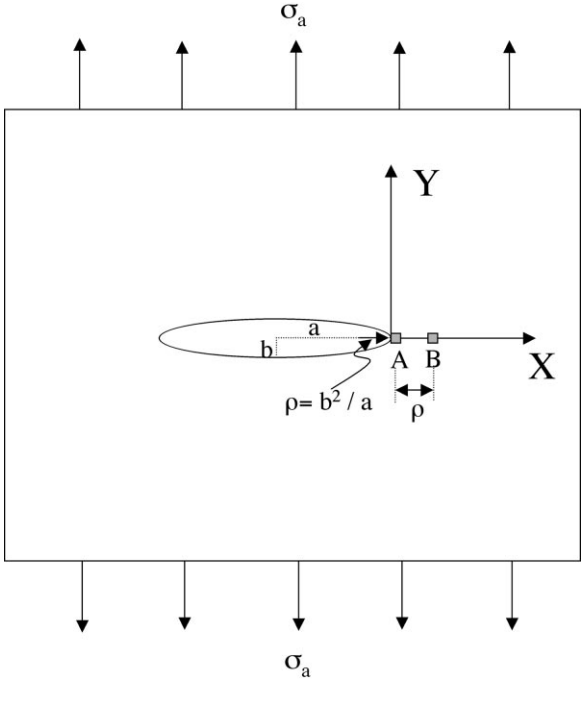

Figure 1
Sketch illustrating an infinite specimen with a notch.

As an introduction to the fracture of a material from a dominant flaw, it is useful to consider an elliptic hole embedded in an isotropic or an orthotropic material under plane strain deformation (Fig. 1). The major and minor axis are represented by a and b, respectively, so that the radius of curvature at the end of the major axis (ρ) is b^2/a. For a far-field applied stress, σ_a, perpendicular to the major axis, the maximum stress σ_{yy} in the loading direction occurs at the crack tip (A), and is given by:

$$\sigma_{yy} = \sigma_a \left(1 + 2\sqrt{\frac{a}{\rho}} \right) \tag{1}$$

for an isotropic material (Timoshenko and Goodier 1951, Inglis 1913), and by:

$$\sigma_{yy} = \sigma_a \left\{ 1 + \sqrt{\frac{a}{\rho}} \left[2 \left(\sqrt{\frac{E_{yy}}{E_{xx}}} - \nu_{yx} \right) + \frac{E_{yy}}{G_{xy}} \right]^{1/2} \right\} \tag{2}$$

for an orthotropic material (Bishop 1972, Green and Taylor 1945), when loaded in one of the material's principal directions. Here E_{xx} and E_{yy} are the elastic moduli in the principal x and y directions, respectively, and G_{xy} is the in-plane shear modulus of the composite. Also, ν_{yx} is the principal Poisson's ratio, equal to the normal contraction in the x direction divided by the tensile elongation in the y direction, when a uniaxial stress is applied in the y direction.

There are two important implications of these results:

(i) In the limit for a sharp crack, when b and ρ approach zero, the stress σ_{yy} at A becomes singular (tends towards infinity). Under this condition, the simple stress-based design concept of a stress concentration factor (SCF) to specify the condition for failure at the crack tip can no longer be used.

(ii) At any value of ρ, the σ_{yy} stress at the notch tip is significantly higher (typically up to 3.5 fold) in a longitudinally loaded unidirectional lamina of comparatively high E_{yy} than in an isotropic material.

Item (i) requires the concepts of fracture mechanics and is treated in greater detail later. However, a few comments regarding item (ii) are worth mentioning here. The higher σ_{yy} stress for a longitudinally loaded unidirectional lamina may imply that it is more susceptible to transverse fracture (fracture plane perpendicular to the fiber axis) than an isotropic material, for the same geometry and far-field applied stress.

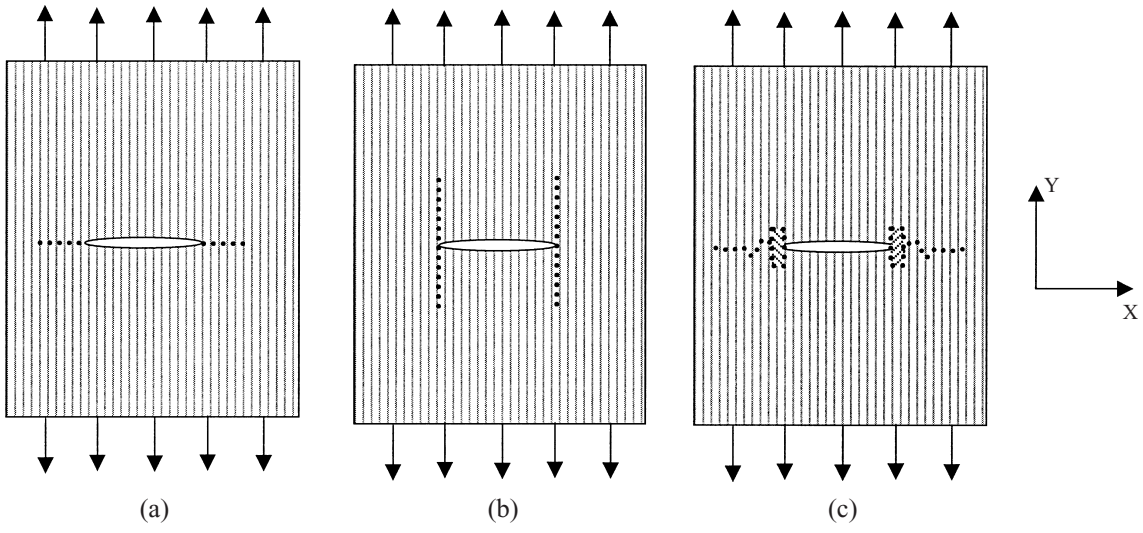

Figure 2
Failure modes in a longitudinally loaded notched/cracked lamina, with the dots indicating the crack extension paths. (a) Crack extension along the original crack plane; (b) damage and crack growth parallel to the loading direction; and (c) damage along the loading direction, followed by tortuous crack growth in an overall direction perpendicular to the loading axis.

However, the anisotropic properties of a unidirectional lamina, primarily the weak strengths in the transverse direction and in shear, introduce crack blunting and stress–relaxation pathways that reduce the level of σ_{yy} ahead of the notch tip. These stress-reduction or crack-shielding mechanisms often make the composite more fracture resistant than the monolithic constituents. Interface mechanics and mechanisms play a critical role in determining the damage tolerance of a composite structure, and are discussed in *Composites: Interfaces* (Cook and Gordon 1964, Kendall 1975, Warrier *et al*. 1997, Gupta *et al*. 1992, He and Hutchinson 1989, Majumdar 1998).

In the case of fracture of a unidirectional lamina with a crack perpendicular to the fiber axis, the unit energy dissipation processes include crack blunting by fiber-matrix delamination, crack bridging by the intact fibers, fiber fracture, matrix plasticity, and crack pinning or trapping. The first tier composite properties, such as the elastic modulus and tensile strength in the principal material directions, dictate how the composite might respond to the presence of a sharp crack. In one case (see Fig. 2(a)) damage may accrue ahead of the notch and lead to crack growth along the original notch/crack plane. Alternatively, if the transverse strength is very low compared to the longitudinal strength, large-scale blunting by splitting along the fiber axis may occur (Fig. 2(b)). The principal stress in the loading direction (σ_{yy}) is thereby relaxed ahead of the crack tip, making the material highly resistant to the propagation of a dominant crack. A low shear strength can also produce a similar blunting effect and contribute to the material's resistance to crack growth. Indeed, some systematic experiments performed by Cooper and Kelly (1967) indicated that if the lamina shear strength was less than 8% of the longitudinal strength, then large-scale shear band growth parallel to the fibers occurred in preference to crack propagation along the original plane of the notch. A more general fracture mode is a combination of damage ahead of the notch in both the x and y directions (Fig. 2(c)), followed by tortuous crack growth in an overall direction perpendicular to the loading axis.

In monolithic materials, the crack path morphology follows that of Fig. 2(a). Ahead of the crack tip, the different stress components then bear a constant ratio to one another as the crack grows, although their overall magnitude increase with crack length; note from Eqn. (1) that the stress σ_{yy} ahead of the crack tip at constant σ_a is proportional to $\sqrt{a}$. This type of crack growth is termed as *self-similar* growth. Alternatively, the crack growth profile in most composites follows Figs. 2(b) and 2(c), where the stress components no longer bear the same ratio with growth of the crack. This loss of self-similarity makes the application of established rules of fracture mechanics rather questionable. However, experimental data indicate that for a given mode of fracture (Fig. 2), the energy required for a significant advance of the initial crack is often characteristic of the material, being only slightly dependent of the specimen geometry. These observations have provided impetus in extending the energy concepts of fracture mechanics, developed primarily for isotropic materials, to composites, thereby allow-

ing a means to assess damage tolerance of a structure in the presence of a notch or a crack-like flaw.

1. Fracture Mechanics Concepts

Fracture of materials can be classified under three major modes of loading, Mode I (or opening mode), Mode II (or in-plane shear mode), and Mode III (or out-of-plane shear mode). Confining attention initially on an isotropic elastic material, the stresses ahead of the crack tip for any combined mode of loading can be expressed as:

$$\sigma_{ij} = \frac{K_{\mathrm{I}}}{\sqrt{2\pi r}} f_{ij}^{\mathrm{I}}(\theta) + \frac{K_{\mathrm{II}}}{\sqrt{2\pi r}} f_{ij}^{\mathrm{II}}(\theta) + \frac{K_{\mathrm{III}}}{\sqrt{2\pi r}} f_{ij}^{\mathrm{III}}(\theta) \quad (3)$$

where r is the radial distance from the crack tip, the $f_{ij}(\theta)$ functions provide an angular dependence, and K_{I}, K_{II}, and K_{III} are the stress intensity factors that characterize the magnitude of the stress singularity for Modes I, II, and III type of loading, respectively (Paris and Sih 1964, Tada *et al*. 1973). In the context of Fig. 1 and Eqn. (1), K_{I} can immediately be identified as $\sigma_{\mathrm{a}}(\pi a)^{1/2}$. The stress intensity factors are related to the elastic energy released per unit advance of the crack tip (designated by the symbol, G) through equations of the form:

$$G_{\mathrm{I}} = \frac{(1-\nu^2)K_{\mathrm{I}}^2}{E} \quad (4)$$

where Eqn. (4) is for a plane strain case and for a pure Mode I type of loading.

Note that K or G characterize the driving force due to an applied load, and can be calculated for any given crack length and load using analytical or computational procedures. Fracture under Mode I loading is postulated to occur when K_{I} or G_{I} reaches a critical value, designated as K_{Ic} and G_{Ic}, respectively, known as the *fracture toughness* of the material. The applicability of this concept in monolithic materials has been validated experimentally using specimens with widely different geometry and crack length. Similar arguments hold good for combined modes of loading, and the effective G is given by:

$$G_{\mathrm{total}} = G_{\mathrm{I}} + G_{\mathrm{II}} + G_{\mathrm{III}} \quad (5)$$

Although K_{Ic} or G_{Ic} can be interchangeably used to characterize the criticality of fracture, they have traditionally involved two modes of thinking. In the case of K, failure is viewed as occurring when a critical stress field is realized ahead of the crack tip. Alternatively, G is most often viewed in terms of the overall energetics of failure, making it more amenable to experimental determination. Thus, it can be shown that G can simply be expressed as:

$$G = \frac{P^2}{2B}\frac{\mathrm{d}C}{\mathrm{d}a} \quad (6)$$

where P is the applied load, C is the specimen compliance, which is a function of crack length a, and B is the specimen thickness.

The lack of self similarity of crack growth in composites makes it difficult to ascribe the onset of crack advance in terms of a defined level of stress field. Alternatively, G_{Ic} retains its significance, in that it still characterizes the level of elastic energy released per unit of crack advance. That is why the energy release rate parameter is most often used in the composites literature, although the K_{Ic} level is also specified through equations of the form shown in Eqn. (5).

There are two additional parameters that become important when inelastic processes dominate. One is the J integral, which is a path-independent integral for any path around the crack tip, and represents the energy associated with a unit advance of the crack tip under situations where stress increases monotonically. Thus, J is quantitatively equal to and synonymous with G for initiation of crack propagation; however, the J integral more rigorously accounts for inelastic processes near the crack tip, and in monolithic materials it characterizes the crack-tip stress and strain fields, similar to K in linear elastic solids.

A final parameter that often enters into fracture mechanics formulations is the crack tip opening displacement (δ), which is the total displacement at the crack tip due to elastic and inelastic deformation processes. In the case of ductile metal alloys, the largest contribution to δ comes from plasticity, and at the onset of fracture it is of the order of distance between precipitates/second phase particles where ductile void nucleation occurs. When plasticity is the dominant inelastic mechanism, δ is related to J through equations of the form:

$$\delta = \frac{kJ}{\sigma_{\mathrm{o}}} \quad (7)$$

where k is of the order of unity, and σ_{o} is the yield strength of the material in uniaxial tension. At the onset of fracture, δ attains a critical value δ_{c} associated with a critical value of J_{Ic} (or equivalently G_{Ic} or K_{Ic})

2. Fracture Mechanisms

Physically δ_{c} represents the blunting of the crack tip due to inelastic deformation. In monolithic materials it ranges from submicron to about 10–20 μm. Alternatively, the crack opening displacements in composites

are much larger due to damage ahead of the crack tip, making the use of conventional fracture mechanics difficult. Unlike highly plastic solids, where the entire structure may behave nonlinearly due to spread of the yield zone, in composites the material behaves elastically in most of the structure, and large nonlinear processes dominate only in the near crack tip region. Therefore, it is convenient to describe the toughness of the composite in terms of a local crack separation law, which now includes all nonlinear effects.

Figure 3 illustrates such a traction law, and the fracture resistance of different composites (PMCs, MMCs, and CMCs) can be traced to variations in this traction law due to different inelastic mechanisms. The area under the curve represents the work of fracture contributed by such a local traction law, and is best designated by its contribution to the energy spent in propagation the crack in the form of parameter ΔG:

$$\Delta G = \int_0^{\delta_c} \sigma(\delta)\,\mathrm{d}\delta \tag{8}$$

In Fig. 3, the rising portion of the curve is due to increasing stresses that take the material point at the crack tip from an initial state to a state of maximum tension. The declining portion is due to different separation mechanisms, such as debonding, pull-out, etc. Most of the analytical formulations in the fracture mechanics of composites deal with the rising portion of the traction separation law, implicitly assuming that there is a vertical drop off to zero load from the point of maximum stress. However, the declining portion can contribute substantially to the work of fracture.

In this section, attention will be concentrated on cracked unidirectional composites loaded in the fiber direction (Figs. 2(a)–2(c)), since the best properties of the composite are obtained in this configuration. Also, at this point it is important to distinguish between different types of systems: (i) brittle matrix system, and (ii) ductile matrix system. The former includes CMCs and PMCs based on brittle polymers like polyimides, while the latter includes MMCs and PMCs that are made with ductile polymers like thermoplastics and toughened resins. This distinction is needed because failure of composites with brittle matrices is preceded by transverse matrix cracks that propagate from the crack/notch tip, leaving intact fibers in their wake. Alternatively, in ductile-matrix systems, it is the fibers that crack first which are then followed by bridging by the ductile matrix. In CMCs, damage tolerance is achieved through a weak fiber-matrix interface. Otherwise, matrix cracks can propagate right through the fiber, making the brittle matrix composite of little engineering value. Energy dissipation in these systems is largely through: (i) crack bridging by the intact fibers, which produce a stress intensity factor (K_B) that opposes the K_{appl} due to the applied load (this is also called crack tip shielding), and (ii) pull-out of cracked fibers, where the fiber cracks are located at some nonzero distance from the crack-plane. In ductile matrix systems, energy dissipation is completely dominated by plastic deformation of the ductile matrix between the cracked fibers. One consequence of this difference is that a higher fiber volume fraction often enhances toughness in brittle matrix systems, whereas it can reduce toughness in ductile matrix systems.

2.1 Brittle Matrix Systems

In terms of the mechanisms of fracture, it is useful to consider the two configurations depicted in Figs. 4(a) and 4(b). These are designated as Case I and Case II, respectively.

In Fig. 4(a), a steady-state condition is considered wherein a single matrix crack emanates from the notch tip at a sufficiently low load. As this matrix crack grows, leaving behind intact fibers, a situation is reached where the fiber at the notch tip just begins to fail. Thereafter, failure of the composite can occur in a steady state manner, and the fracture toughness corresponds to the applied stress intensity factor at which lead fiber fails. The toughening associated with Case I has been worked out by Budiansky and Amazigo (1989). In Case II, we consider fracture of fibers that have a statistical strength distribution so they fail at different distances from the crack plane. Final failure requires that these fibers pull-out of the matrix. Because of frictional resistance, substantial energy is dissipated in the decreasing segment of the stress-displacement traction law (Fig. 3), contributing to significant increase in the toughness of the composite. The work of pull-out has been worked out by a number of investigators (Kelly 1970, Phillips 1972), and we present here the results of Thouless and Evans (1988).

(*a*) *Case I.* As shown in Budiansky and Amazigo (1989), a simple J integral calculation provides the following relationship:

$$\frac{J_{\text{applied}}}{A} = (1-c)\,J_{\text{matrix}} + \int_0^{\delta_c} \sigma(\delta)\,\mathrm{d}\delta \tag{9}$$

where c is the volume fraction of fibers, A is a factor that accounts for the orthotropy of the sheet in Fig. 4(a) ($= 1.0$ for identical elastic constants of the fiber and the matrix), $J_{appl} = (1-\nu^2)K^2_{applied}/E_c$, and $J_{matrix} = (1-\nu^2)K^2_m/E_m$, where K_m is the critical stress intensity factor for the monolithic matrix. Also, E_m is the modulus of the matrix, and E_c is the composite longitudinal modulus ($= cE_f + (1-c)E_m$, where E_f is fiber modulus). Values of A as a function of c and E_f/E_m are plotted in Budiansky and Amazigo (1989). Note that J is synonymous with G, but is more

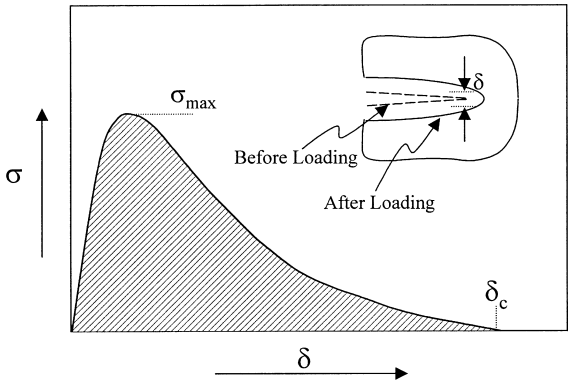

Figure 3
Stress-displacement traction law.

appropriate here because of inelastic processes. Also, if there are parallel matrix cracks emanating from the notch tip, then the first term in Eqn. (9) is multiplied by the number of those matrix cracks.

Assuming relative sliding/slipping between the cracked matrix and the intact fibers in the wake of the matrix crack, it follows that:

$$\frac{J_{\text{applied}}}{J_{\text{matrix}}} = A(1-c)\left[1+\frac{2c\sigma_{\text{f}}^{\text{avg}}}{\sigma_{\text{ss}}}\right] \tag{10}$$

where $\sigma_{\text{f}}^{\text{avg}}$ is the average bundle strength of the fiber, and σ_{ss} is the steady-state matrix cracking stress (sometimes referred to as the pseudo yield stress) for the composite. As shown in the ACK theory (Aveston, Cooper, and Kelly 1971), and also analyzed in the BHE theory (Budiansky, Hutchinson, and Evans 1986) σ_{ss} can be represented as:

$$\sigma_{\text{ss}} = E_{\text{c}}\left[\frac{6c^2E_{\text{f}}\tau}{(1-c)E_{\text{c}}E_{\text{m}}}\right]^{1/3}\left[\frac{J_{\text{matrix}}}{rE_{\text{m}}}\right]^{1/3} \tag{11}$$

where τ is the axial frictional sliding stress between the fiber and the matrix, and r is the radius of the fiber. Note that $c\sigma_{\text{f}}^{\text{avg}}$ is approximately the breaking strength of an unnotched longitudinal composite, since only the fibers carry the entire load after matrix cracks run through the entire length of the composite at a stress of σ_{ss}. A typical value of $c\sigma_{\text{f}}^{\text{avg}}/\sigma_{\text{ss}}$ is five, so that Eqn. (10) indicates that a 10-fold toughness increase is obtainable based on this mechanism of toughening.

It is useful to note that the toughness ratio varies inversely as σ_{ss} (Eqn. (10)). Thus, while a higher frictional resistance (τ) and a smaller fiber radius (r) would increase the "yield strength" of the brittle matrix composite, it is detrimental to the fracture toughness. Consequently, material design will need to be optimized, depending upon the desired application in components.

(*b*) *Case II*. In this case, we consider the statistical failure of brittle fibers, whose strength can be expressed by the two-parameter Weibull distribution. In this methodology, the cumulative probability of failure (P_{f}) of a fiber at a stress σ is given by:

$$P_{\text{f}} = 1-\exp^{-(L/L_0)(\sigma/\sigma_0)^m} \tag{12}$$

Here σ_{o} is the characteristic fiber strength at length L_{o}, and is usually designated as the Weibull strength, and m is the Weibull modulus.

The problem of Fig. 4(b) was analyzed by Thouless and Evans (1988). Figure 5 from Evans (1990) shows the traction law, in nondimensional co-ordinates, that result for different values of Weibull modulus, m. Here a value of infinity corresponds to a deterministic strength (similar to Case I), and may occur in epoxy based composites toughened with polymeric fibers, or even with SiC fibers ($m \sim 15$ in the virgin condition). Alternatively, a value of $m = 5$ more closely resembles situations that may be encountered in CMCs. Note that as m decreases, the declining portion of the traction law contributes more and more to the toughness of the composite. In terms of the design parameters, the toughness increase is approximately proportional to $\{r^{m-3}/\tau^{m-1}\}^{1/(m+1)}$. Thus, the toughness increases with increasing fiber radius when $m > 5$, but decreases when $m < 3$. Conversely, it increases with increasing τ when $m < 1$, and decreases when $m > 2$. This type of behavior arises because of the competing importance of the contribution to toughness from intact bridging fibers and the failed fibers that experience pull out. Thus, knowledge of m and τ are important for optimization of composite toughness under fiber pull-out conditions.

(*c*) *Case of ductile fiber toughening in brittle matrix composites*. This type of toughening mechanism, although developed for particle toughened composites, is also applicable for ductile fiber toughened CMCs and PMCs. Under the condition that the ductile fiber is perfectly plastic and fully yielded ($\sigma = \sigma_{\text{Y}}$), Eqn. (8) shows that the toughening contribution per ductile fiber is simply $k\sigma_{\text{Y}}\delta_{\text{c}}$, where k accounts for a higher strength of the constrained ductile fiber. Assuming no debonding between the cracked matrix and the ductile fiber (for example, a metallic fiber), the value of δ_{c} is of the order of the fiber diameter, $2r$. The value of k is more difficult to estimate, but should not exceed that ahead of a crack tip, namely 3–4σ_{Y}. These parameters then allow a fair assessment of toughening associated with ductile fibers in a brittle matrix. A more rigorous treatment (Budiansky *et al.* 1988) leads to the result:

$$\frac{K_{\text{applied}}/K_{\text{m}}}{\sqrt{\bar{\omega}(1-c)}} = \left[1+\frac{2c}{1-c}\frac{E_{\text{m}}S\delta_{\text{c}}}{K_{\text{m}}^2(1-\nu_{\text{m}}^2)}\right]^{1/2} \tag{13}$$

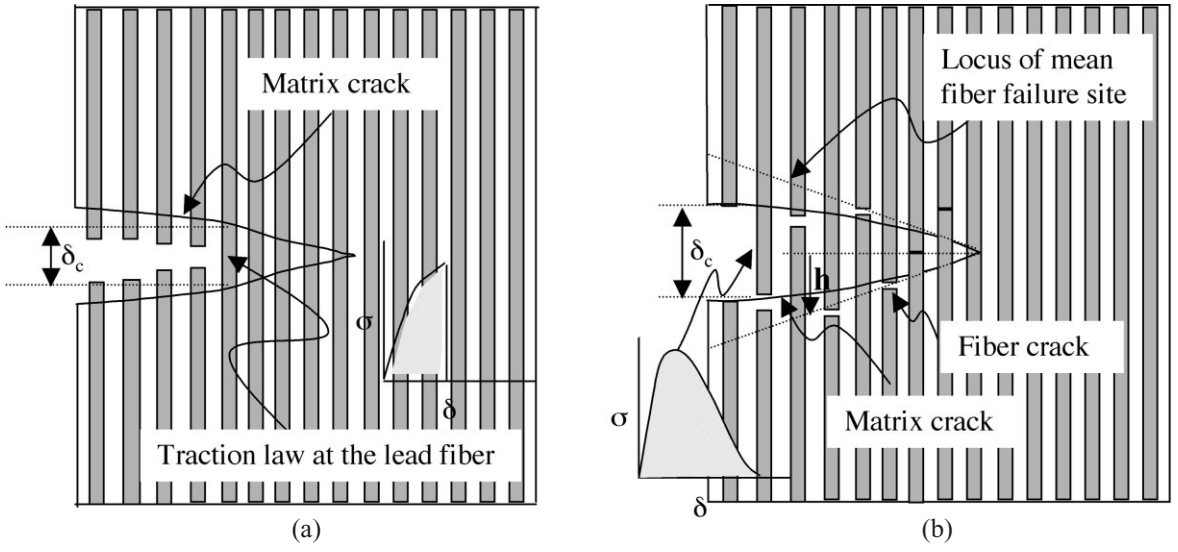

Figure 4
Crack propagation in brittle matrix composites. (a) Steady-state bridging of matrix cracks by intact fibers, with the lead fiber failing at the original crack plane. (b) Matrix crack bridging, but in this case the fibers fail statistically at different distances from the crack plane. The traction law is sketched for the two cases.

where S is the effective strength of the ductile fiber and c is fiber volume fraction. Also,

$$\varpi = \frac{E_c(1-\nu_m^2)}{E_m(1-\nu_c^2)} \tag{14}$$

It is useful to note that substantial increase in δ_c is possible if there is relative sliding between the fiber and the matrix, since bridging can be sustained over much larger matrix crack length. Essentially, δ_c becomes the gage length over which the debonding occurs, times the strain to failure in uniaxial tension. However, S is close to σ_Y in this case, so that there is substantial loss of stiffness of the system in the presence of matrix cracks. Since component functionality is also often based on maximum possible displacement, there will always be a need to optimize the interface for component specific performance.

2.2 Ductile Matrix Systems

In ductile matrix systems, a number of different behaviors have been observed depending on the strength of the matrix, the fiber-matrix bond strength, and the volume fraction of fibers.

When the matrix strength is low, matrix dominated shear deformation occurs prior to any fiber fracture. Indeed, in boron fiber reinforced aluminum composites, a deformation mode similar to Fig. 6 is observed (Dvorak *et al.* 1989, Awerbuch and Hahn 1979, Reedy 1980), where an intense slip zone develops over a plastic zone of length (R) perpendicular to the crack plane. At a critical load, when R is on the order of 3–17-fold the crack length, the damage zone stops propagating and is replaced by failure of fibers at the crack tip. This, in turn leads to catastrophic fracture of the composite along the original notch plane. Most notable is the fact that the H-shaped shear zone is created prior to crack extension, and is absent during propagation of the crack, i.e., crack extension is non self-similar. A similar type of damage zone and crack extension has also been observed in glass fiber reinforced epoxy composites (Tirosh 1973).

In the above type of deformation mode, the effective toughening is extremely high, because the blunted crack tip attenuates the stress ahead of the crack tip over a distance of the order of the crack tip opening displacement. For crack lengths of a few millimeters or longer, toughness values of $100\,\mathrm{MPa\,m^{1/2}}$ have been realized for the B/Al system. The effect reduces at smaller crack length, and approaches approximately $30\,\mathrm{MPa\,m^{1/2}}$ at crack length $< 0.5\,\mathrm{mm}$. Thus, fracture toughness may not be the appropriate parameter for predicting failure in these systems which do not obey self-similar crack growth. Dvorak *et al.* (1989) attempted to estimate the onset of fracture based on attainment of a critical strain in the fiber direction over two fiber diameter distance ahead of the crack tip. It was found that the local strain in the representative volume element for specimens with different notch lengths all fall in the error band for the failure strain of unnotched composites. The following set of equations may be used to estimate the failure load (P_{ult}) for a

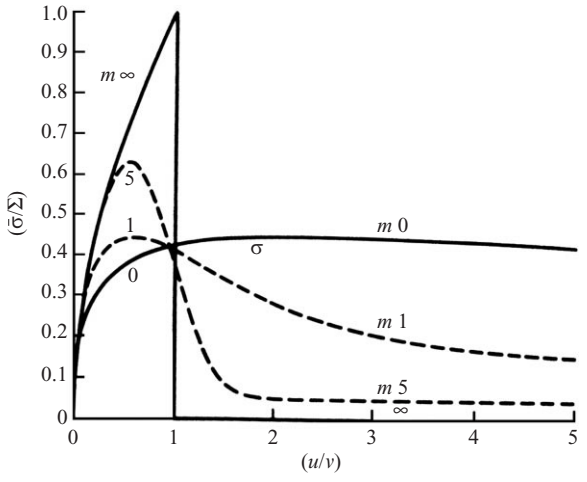

Figure 5
Nondimensional traction law (σ versus u) for the pull-out fiber case, for different values of Weibull modulus, m (after Evans 1990).

center-cracked panel of width W and crack length $2a$ (Zarzour and Paul 1992), and possessing an unnotched strength, $\sigma_{\text{unnotched}}$:

$$\frac{P_{\text{ult}}}{\left(1-\dfrac{2a}{W}\right)}+2\frac{\tau^*}{\pi(a_2-a_1)}\left[-a_1^2\ln\left(\frac{1+\sqrt{1+a_1^2\beta^2}}{a_1\beta}\right)\right.$$
$$\left.+a_2^2\ln\left(\frac{1+\sqrt{1+a_2^2\beta^2}}{a_2\beta}\right)\right]=\sigma_{\text{unnotched}} \qquad (15)$$

where

$$a_{1,2}^2=\left(\frac{E_1}{2G_{12}}-\nu_{12}\right)\pm\sqrt{\left(\frac{E_1}{2G_{12}}-\nu_{12}\right)^2-\frac{E_1}{E_2}} \qquad (16)$$

and

$$b\approx d\left(\frac{2\pi}{3\sqrt{3}c}\right)^{1/2} \qquad \beta=\frac{aP_{\text{ult}}}{b\tau^*}$$

Here, d is the fiber diameter, c is the volume fraction of fibers, τ^* is the in-plane shear strength of the unidirectional composite in the fiber direction, E_1 is the modulus in the fiber direction, E_2 in the transverse direction, G_{12} is the shear modulus, ν_{12} is the Poisson's ratio, and b is of the order of distance between two adjacent fibers.

When the matrix strength is high, or the fiber volume fraction is high, the dominant damage mode is fiber fragmentation in the zone of intense matrix plastic deformation near the crack tip, and ultimately composite fracture. This is illustrated in Fig. 7(a). In

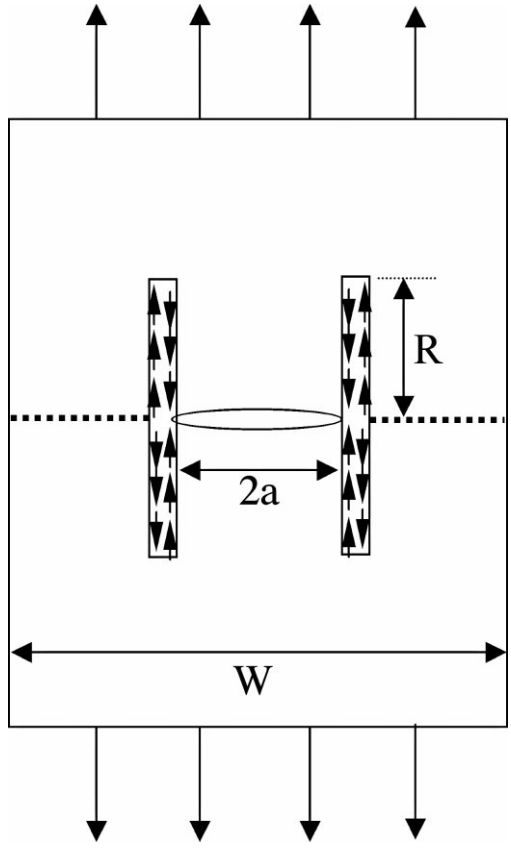

Figure 6
Sketch illustrating H-type plastic zone development at the notch tip, followed by composite fracture along original notch plane.

order to predict the fracture toughness, some estimate of the flow stress and the critical displacement is needed, for plugging into Eqn. (8). Friler *et al.* (1993) and Argon (2000) modeled the failure process by considering that the periphery of fractured fiber tips act as the nucleation center from which intense matrix plasticity develops (see Fig. 7(b)). This is a form of macroscopic void growth, at a length scale that is significantly larger than the distance between intermetallic particles, which act as the void nucleation site for fracture of monolithic metallic alloys. Using Eqn. (8), Friler *et al.* (1993) estimate the fracture toughness as:

$$J_{\text{Ic}}\approx\frac{1}{\sqrt{3}}(1-c)\sigma_{\text{Y}}\text{L}_{\text{D}} \qquad (17)$$

where

$$L_{\text{D}}\approx\beta_{\text{n}}d\frac{1-\sqrt{c}}{\sqrt{c}} \qquad (18)$$

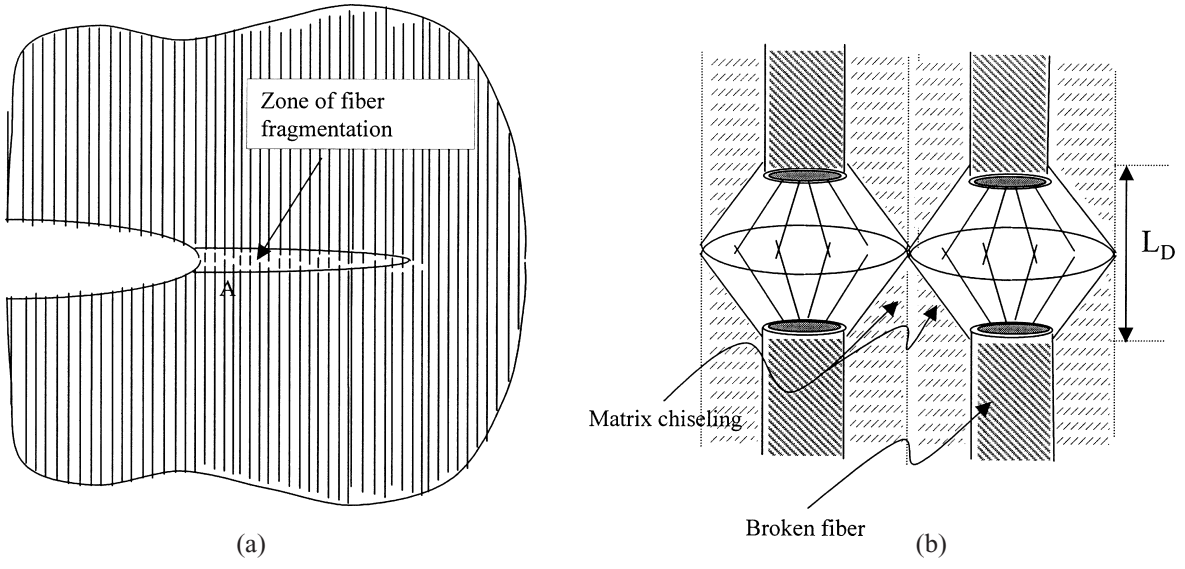

Figure 7
(a) Overall damage pattern in ductile matrix composites. There is a zone of plasticity where fibers are fragmented, followed by propagation of the matrix crack through that damaged region. (b) The Friler model for determining the toughness, assuming chiseling of the matrix from the broken fiber ends (Friler *et al*. 1993).

and β_n is approximately 2. Here d is the diameter of the fiber, c is the volume fraction of fibers, and σ_Y is the yield stress of the matrix.

Very few experiments have been conducted on the fracture toughness of titanium matrix composites. Connell *et al*. (1994) reported a toughness of approximately $71\,kJ\,m^{-2}$ for a SiC/Ti-alloy, which may be compared with a typical toughness of $40\,kJ\,m^{-2}$ (based on $K_{Ic} = 70\,MPa\,m^{1/2}$) for monolithic Ti–6Al–4V alloy. Using Eqn. (17) with $\sigma_Y = 1040\,MPa$, $c = 0.32$, and $d = 100\,\mu m$, a toughness value of $62\,kJ\,m^{-2}$ is estimated, which compares reasonably well with the experimental data.

It is useful to note that J_{Ic} predicted by Eqns. (17) and (18) is quite strongly dependent on the volume fraction of fibers. Thus, $(1-c)(1-\sqrt{c}/\sqrt{c})$ decreases from approximately 0.59 to 0.12 on increasing the volume fraction from 0.3 to 0.6. High volume-fraction alumina/aluminum composites are currently being developed for a variety of applications, such as high-tension electrical cables and piston rods. Because of the lower strength of the alloy, and the high volume fraction of alumina fibers, toughness values significantly less than titanium matrix composites are anticipated.

A final note is in order regarding the role of the fiber-matrix interface. Equation (17) shows that the toughness is an increasing function of L_D. Weak interfaces would permit greater fiber-matrix sliding, thereby increasing the fracture toughness. This effect was elegantly utilized by Argon *et al*. (1998) to toughen aluminum-based composites, while maintaining acceptable transverse strengths. In SiC reinforced titanium matrix composites, pull-out lengths are typically less than one fiber diameter, even for weak carbon based interfaces. This is largely because of the high radial compressive stress that is generated at the fiber-matrix interface at the tip of a cracked fiber. For strong interfaces, such as those formed without a carbon layer on the SiC monofilaments, the pull-out length will be even shorter. However, the effect of a smaller L_D may be balanced by a higher flow stress associated with constrained yielding of the matrix in the fragmentation zone. Tensile tests on unnotched SiC/Ti-matrix composites with different interfaces indicate correlated fiber fractures, independent of the type of interface. Slip band observations and ultrasonic images of fiber breaks confirm that correlated fractures are a result of slip band interactions, whereby a slip band impinging on a fiber localizes sufficient strain to fracture that fiber (Majumdar *et al*. 1998). Similar experiments have to be conducted with notched composites to provide an assessment of the role of interface strength on the toughness of composites with high matrix strength.

2.3 Intermediate Ductility Matrix Systems

An important characteristic of polymer matrix composites is that their behavior can range from brittle to ductile matrix systems depending on the particular polymer used. Moreover, changing the temperature or loading rate (loading history) will alter the ductility for

any polymer. Higher temperatures and/or lower loading rates generally increase ductility. Both the amount of ductility and the dependence on temperature and loading history are determined by the microstructure of the polymer. This includes molecular level structure as well as morphology since many polymer matrices are two phase systems where the base polymer contains particles of a polymeric additive to improve toughness and other desirable properties. In a sense, the polymer itself is a composite.

The relationship between microstructure and ductility of polymers has been studied extensively, but is beyond the scope of this article. The reader is referred to some of the many references in this area (Bucknall 1977, Bitner *et al*. 1981, Pearson and Yee 1989, Wu *et al*. 1990, Huang *et al*. 1993, Kinloch *et al*. 1983). What should be noted here, however, is that the effect of polymer ductility on matrix toughness can often be described in terms of a toughening mechanism involving crack tip blunting, see Eqn. (7). Thus, increasing the ductility allows more blunting of the crack tip. This, in turn, reduces the local stress concentration, thereby postponing damage initiation and retarding damage growth. The ultimate result is increased fracture toughness of the polymer. Kinloch *et al*. (1983) have investigated this mechanism, by plotting the toughness of the polymer as a function of crack tip radius, where the radius was obtained either by blunting of an initially sharp crack or by incorporating artificially drilled holes of fine enough radius at the end of a sharp notch. Specimens with sharp cracks were tested at different temperatures and cross-head speeds to vary the amount of blunting, while specimens with the artificial crack tip radii were loaded at high cross-head speeds to minimize further blunting of the crack tip. A clear relationship between the measured toughness and the root radius was found, but more importantly the behavior was independent of how the tip radius was incorporated into the specimen.

In addition to crack blunting, three other toughening mechanisms are also important in polymer composites: crack pinning, crack diversion or bifurcation, and crack bridging. The interaction of these mechanisms can be illustrated by considering the two most common forms of composites fracture in PMCs, i.e., interlaminar and transverse.

(*a*) *Interlaminar fracture*.

Crack Blunting: In interlaminar fracture, the crack propagates in the resin and/or at the resin-fiber interface parallel to the fibers. As a result, the matrix toughness would be expected to play a major role in the interlaminar fracture energy. One example of this is shown in Fig. 8 where the Mode I interlaminar fracture energy is plotted versus the Mode-I fracture toughness of the ''neat'' resin (i.e., the unreinforced matrix) (Hunston *et al*. 1987). The results show that tougher resins produce tougher composites, but the relationship is not a simple one; see the trend lines in Fig. 8. In the brittle range, the composite is significantly tougher than the resin so the transfer of toughness is good. Beyond a certain point, however, the transfer is less complete. To increase the fracture energy of the composite by $1\,J\,m^{-2}$, the fracture energy of the resin must be increased by approximately $2\,J\,m^{-2}$. The proposed explanation is that all crack blunting mechanisms involve inelastic deformation of the matrix material in the crack-tip region, with the toughness increasing with the size of the plastic/viscoplastic zone, consistent with elastic-plastic fracture mechanics principles. For brittle materials, this inelastic zone is smaller than the inter-fiber spacing, so that the resin toughness is completely transferred to the composite. For tougher materials, however, the size of the inelastic zone in the bulk resin is larger than the inter-fiber spacing. Consequently, in the interlaminar fracture experiment, the fibers limit the extent of toughness increase per unit increase in resin toughness. In support of this argument, the estimated size of the deformation zone at the transition point in behavior (intersection of the trend lines in Fig. 8) compare very well with the interfiber spacing between plies.

Crack Pinning or Trapping: Because interlaminar fracture is an important failure mode in polymeric systems, methods have been developed to improve the fracture toughness. One approach is to add rubber particles between the fiber layers during fabrication. The particles are thereby trapped between the fiber layers and form a barrier to crack propagation. When an interlaminar crack propagates it runs into these barriers and is held back because the particles have a higher fracture toughness than the matrix. In effect, the matrix crack is pinned or trapped by these barriers. Higher loads are then required to force the crack through or around the particles. This toughening mechanism has been shown to be effective even for impact loading indicating that the pinning mechanism is relatively independent of loading rate. This is in contrast to the case of the crack blunting mechanism, where the toughness is significantly rate sensitive. Bower and Ortiz (1990) have modeled the crack trapping behavior and have shown good correlation with experimental results.

Crack Diversion or Bifurcation: It was proposed in some early studies of interlaminar fracture that under the proper conditions, poor fiber-matrix bonding could increase the fracture energy (McKenna *et al*. 1974). For this to occur, the weak interface bonding needed to be localized, randomly distributed along the fibers, and interspersed with areas of good bonding. Under these conditions, a growing crack would be diverted back and forth between the many weakly bonded areas so that the trajectory became very tortuous. Moreover, the crack may be split into several branches that grow for a short distance and then end. When poor interface bonding becomes too extensive,

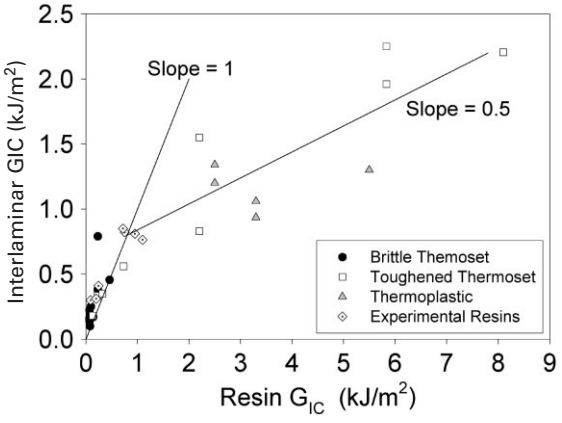

Figure 8
Composite interlaminar fracture energy as a function of the fracture energy for the corresponding resin. Lines indicate the general trends only. The relative standard uncertainty in the determination of G_{Ic} is 15% (after Hunston *et al.* 1987).

however, the result is a decrease in fracture toughness because the weak interface provides an easy path for crack growth. This is illustrated in Fig. 8 where the thermoplastic resins generally show lower interlaminar fracture toughness than thermoset resins with the same resin fracture energies. Examination of the fracture surface shows that the fiber-matrix interface bonding in the thermoplastics was much poorer than it was in the corresponding thermoset.

Crack Bridging: Another interesting feature in Fig. 8 is that the interlaminar fracture energy for composites with the more brittle resins is almost always higher than the fracture energy for the resin itself. This has been attributed to the fact that the composite has an additional toughening mechanism: fiber bridging (Hunston *et al.* 1987), discussed earlier in this article.

(*b*) *Longitudinal fracture*. These same four types of toughening mechanisms are present when a crack propagates perpendicular to the fibers. As discussed previously, toughening involves a combination of work associated with interface debonding, the work of stretching and breaking fibers, and the work required for fiber pull-out.

With polymers, experiments generally show that the highest resistance to crack growth occurs at intermediate bond strength. Moreover, with very strong interface bonding, a post failure examination shows relatively few fiber ends protruding from the fracture surface. As the interface bond strength decreases, there is an increase in the number of protruding fiber ends and their length. The authors (Kelly 1970, Harris *et al.* 1975) explain these results by noting that when the interface bond is strong, there is resistance to crack diversion and fiber-matrix debonding, and the matrix crack can propagate into the fiber. Consequently, fewer fibers protrude on the fracture surface. As the interface strength is decreased, the amount of crack diversion and interface debonding increases, so that fiber fractures can now occur statistically at locations away from the crack plane. Consequently, there is an increase in energy dissipation due to both debonding and pull-out, consistent with Figs. 3 and 5. However, when the interface strength becomes very low, the work of debonding may actually decrease even with a greater length of debonding, because of lower frictional resistance per unit area of the fiber-matrix interface. For polymer matrix systems, the frictional resistance is quite low, indicating that below a certain bond strength the pull-out energy could also decrease with a decrease in interface strength. Consequently, the highest fracture energy is obtained at an intermediate value of interface strength.

3. *Concluding Remarks*

Although the variety of composite materials is very large, fracture mechanics provides a common approach to analyze failure. Examining the similarities and differences among the various types of composites shows that the toughening mechanisms often extend across a wide range of composites. Consequently, much can be learned from such studies. In order to design composites intelligently, it is important to develop predictive equations based on the observed micromechanisms of fracture. Such models have to be validated experimentally, and this article illustrates a number of examples where good correlations between experiments and model predictions have been obtained. For additional reading, please refer to Kelly and Macmillan (1986).

Bibliography

Argon A S 2000 Fracture: strength and toughness mechanisms. In: Kelly A, Zweben C (eds.) *Comprehensive Composite Materials*, Vol. 1. Pergamon, Oxford, pp. 763–802

Argon A S, Seleznev M L, Shih C F, Liu X H 1998 Role of controlled debonding along fiber/matrix interfaces in the strength and toughness of metal matrix composites. *Int. J. Fract.* **93**, 351–71

Aveston J A, Cooper G A, Kelly A 1971 Single and multiple fracture. In: *Properties of Fibre Composites*. IPC Science and Technology, Guildford, UK, pp. 15–26

Awerbuch J, Hahn H T 1979 Crack tip damage and fracture toughness of boron/aluminum composites. *J. Compos. Mater.* **13**, 82–107

Bishop S M Stresses near an elliptical hole in an orthotropic sheet. Technical Report 72026. Royal Aircraft Establishment, Farnborough, UK

Bitner J L, Rushford J L, Rose W S, Hunston D L, Riew C K 1981 Viscoelastic fracture of structural adhesives. *J. Adhes.* **13**, 3–28

Bower A F, Ortiz M 1990 Solution of 3-dimensional crack problems by finite perturbation methods. *J. Mech. Phys. Solids* **38**, 443–80

Bucknall C B 1977 *Toughened Plastics*. Applied Science, London

Budiansky B, Amazigo J C 1989 Toughening by aligned, frictionally constrained fibers. *J. Mech. Phys. Solids* **37** (1), 93–109

Budiansky B, Amazigo J C, Evans A G 1988 Small-scale crack bridging and the fracture toughness of particulate reinforced ceramics. *J. Mech. Phys. Solids* **36** (2), 167–87

Budiansky B, Hutchinson J W, Evans A G 1986 Matrix fracture in fiber-reinforced ceramics. *J. Mech. Phys. Solids* **34**, 167–89

Connell S J, Zok F W, Du Z Z, Suo Z 1994 On the tensile properties of a fiber reinforced titanium matrix composite—II. Influence of notches and holes. *Acta Metall.* **42** (10), 3451–61

Cook J, Gordon J E 1964 A mechanism for the control of crack propagation in all-brittle systems. *Proc. R. Soc. London* **A282**, 508–20

Cooper G A, Kelly A 1967 Tensile properties of fiber-reinforced metals: fracture mechanics. *J. Mech. Phys. Solids* **15**, 229–79

Dvorak G J, Bahei-El-Din Y A, Bank L C 1989 Fracture of fibrous metal matrix composites—I. *Experimental results. Eng. Fract. Mech.* **34** (1), 87–123

Evans A G 1990 The mechanical behavior of ceramic composites. In: Embury, J D, Thompson A W (eds.) *The Modeling of Material Behavior and Its Relation to Design*. Proc. TMMS Symp. TMMS, Warrendale, pp. 245–67

Friler J B, Argon A S, Cornie J A 1993 Strength and toughness of carbon fiber reinforced aluminum matrix composites. *Mater. Sci. Eng.* **A162**, 143–52

Green A E, Taylor G I 1945 *Proc. R. Soc. London* **A184**, 181

Gupta V, Argon A S, Suo Z 1992 Crack deflection at an interface between two orthotropic media. *J. Appl. Mech., Trans. ASME* **59**, S79–87

Harris B, Morley J, Phillips D C 1975 Fracture mechanisms in glass-reinforced plastics. *J. Mater. Sci.* **10**, 2050–61

He M Y, Hutchinson J W 1989 Crack deflection at an interface between dissimilar elastic materials. *Int. J. Solids Struct.* **25**, 1053–67

Huang Y, Hunston D L, Kinloch A J, Riew C K 1993 Mechanisms of toughening thermoset resins. In: Riew C K, Kinloch A J (eds.) *Toughened Plastics* I. Advances in Chemistry Series 233. American Chemical Society, Washington, DC, pp. 1–35

Hunston D L, Moulton R J, Johnston N J, Bascom W D 1987 In: Johnston N J *Toughened Composites*, ASTM STP 937. American Society for Testing and Materials, Philadelphia, pp. 74–94

Inglis C E 1913 *Trans. Inst. Nav. Archit.* **55**, 219

Kelly A 1970 Interface effects and the work of fracture of a fibrous composite. *Proc. R. Soc. London* **A319**, 95–116

Kelly A, Macmillan N H 1986 *Strong Solids*, 3rd Edn. Clarendon, Oxford

Kendall K 1975 Transition between cohesive and interfacial failure in a laminate. *Proc. R. Soc. London* **A344**, 287–302

Kinloch A J, Shaw S J, Todd D A, Hunston D L 1983 Deformation and fracture behavior of a rubber toughened epoxy. *Polymer* **24**, 1341–63

Majumdar B S, Matikas T E, Miracle D B 1998 Experiments and analysis of single and multiple fiber fragmentation in SiC/Ti-6Al-4V MMCs. *Composites B* **29**, 131–45

Majumdar B S 1998 Fiber-matrix interface. In: Mall S, Nicholas T (eds.) *Titanium Matrix Composites*. Technomic, Lancaster, PA, pp. 113–68

McKenna G B, Mandell J F, McGarry F J 1974 Interlaminar strength and toughness of fiberglass laminates. In: *Proc. SPI Annu. Tech. Conf. RPD*, Society of Plastics Industries, New York, pp. Sect. 13-C

Paris P C, Sih G C 1964 Fracture toughness testing and its applications. ASTM STP 381. American Society for Testing and Materials, Philadelphia, pp. 30–81

Pearson R A, Yee A F 1989 Toughening mechanisms in elastomer modified epoxies—III: effect of cross-link density. *J. Mater. Sci.* **24**, 2571–80

Phillips D C 1972 The fracture energy of carbon fiber reinforced glass. *J. Mater. Sci.* **7**, 1175–91

Reedy E D 1980 Analysis of center notched monolayers with application to boron/aluminum composites. *J. Mech. Phys. Sol.* **28**, 265–86

Tada H, Paris P C, Irwin G 1973 *The Stress Analysis of Cracks Handbook*. Del Research Corporation, Hellertown, PA

Thouless M D, Evans A G 1988 Effects of pull-out on the mechanical properties of ceramic-matrix composites. *Acta Metall.* **36** (3), 517–22

Timoshenko S, Goodier J N 1951 *Theory of Elasticity*, 2nd Edn. McGraw Hill, New York

Tirosh J 1973 The effect of plasticity and crack blunting on the stress distribution in orthotropic composite materials. *J. Appl. Mech., Trans. ASME* **40**, 785–90

Warrier S G, Majumdar B S, Miracle D B 1997 Interface effects on crack deflection and fiber bridging behavior during fatigue crack growth in titanium matrix composites. *Acta Metall.* **45** (12), 4969–80

Wu W L, Hu J, Hunston D L 1990 Structural heterogeneity in epoxies. *Polym. Eng. Sci.* **30** (14), 835–40

Zarzour J F, Paul A J 1992 On plastic zones and fracture strengths in some metal matrix composites. *J. Mat. Eng. Perform.* **1** (5), 659–68

B. S. Majumdar and D. Hunston

Encyclopedia of Materials: Science and Technology
ISBN: 0-08-0431526
pp. 1618–1629